

Exoplanet detection of a K2 Hot Jupiter Object

Ansh R. Gupta

1. INTRODUCTION

Exoplanet astronomy has remained among the most active and publicly known subfields of astronomy for multiple decades. The study of exoplanets has the potential to uncover signatures of extraterrestrial lifeforms, but its applications reach far beyond this imperative. Possible results include the discovery of habitable planets, refinement of observational and data reduction techniques applicable to other fields, and insight into the formation of the Solar System. This research focused on the transit method, using photometry to obtain a light curve of the target star and detect the presence of an exoplanet. The transit method is applicable for systems with an inclination near 90 degrees, meaning that the plane of the system is nearly along the line of observation. For these systems, exoplanets may briefly complete a transit of the target star at periodic intervals, observable as a characteristic dip in the brightness of the system. By measuring flux from candidate systems over a transit, one can obtain a light curve to determine physical properties and orbital parameters of a potential exoplanet. If repeated observations of transit light curves reveal consistent results, a candidate can be confirmed as an exoplanet. The K2-45 system was first observed by the Kepler Space Telescope K2 mission ([Vanderburg et al. 2016](#)). The host star is a spectral type K star similar to the Sun, located roughly 1600 lightyears away ([Gaia Collaboration et al. 2018](#)). According to data from the NASA exoplanet archive ([Ciardi 2021](#)), K2-45 b is a confirmed roughly Jupiter-sized exoplanet orbiting at less than 1/15 the distance of Mercury from the Sun. These “Hot Jupiters” are over-represented in surveys due to the large fraction of light blocked during transit (transit depth). We selected K2-45 b as a target due to its high transit depth, relatively high elevation, and adequate distance to the moon on the night of the observation. In this project, we aimed to observe a transit light curve of the target system, generate a transit model using the batman python package ([Kreid-](#)

berg 2015), and fit the model to the observed data to extract planet and orbital parameters for the system. We present our findings here and compare our values with those in the literature.

2. OBSERVATIONS AND DATA ANALYSIS

2.1 Telescope and CCD Properties

Observations were made using the 61" Kuiper telescope on Mount Bigelow, a peak in the Santa Catalina Mountains of Southern Arizona. The primary mirror of the telescope has a diameter of 1.54 m, with a primary focal ratio f/4. The telescope is equipped with a Fairchild CCD486 4Kx4K CCD, known as the Mont4K SN3088, which has a size of 4096x4097 pixels with 15 micron pixels split over two halves, an image scale of 0.14 arcsec/pixel, and a 580 x 580 arcsec² field of view. Measured characteristics include a gain of 3.1 electrons/ADU, readout noise of 5.0 electrons, dark current of 16.6 electrons/pixel/hour, and full well of 131,000 electrons unbinned (Smith 2022). The CCD operating temperature of -130 °C and camera temperature of -117 °C were maintained by a liquid nitrogen filled Dewar. Pre-observation images taken by Dr. Elizabeth Green revealed that K2-45 was brightest under the WFPC2 F606W filter, but the greater number of sky counts compared to the Harris R filter may have impacted the visibility of nearby fainter reference stars. Since the moon was not up for our observations, the number of counts from the target star was large enough to allow for observation in the R band, increasing the relative brightness of desired reference stars. Other filters were ruled out due to fringing effects from the CCD.

2.2 Observation

Non-essential access to the telescope has been limited in order to limit potential exposure to COVID-19, so observations were directly carried out by Dr. Elizabeth Green while group members were present online via Zoom video conferencing software. Telescope calibration was carried out by Dr. Green before the observations, including the capture of a bias and flat field image. Throughout the observation, the sky was relatively clear, with minimal to no cloud cover and relatively low wind speed of 2-7 mph from the SSW. Dr. Green noted sporadic gusts of 10-12 mph, so windscreens were raised to contain the impacts of vibrations from wind. Overall seeing was reported as 1.7" – 2.2".

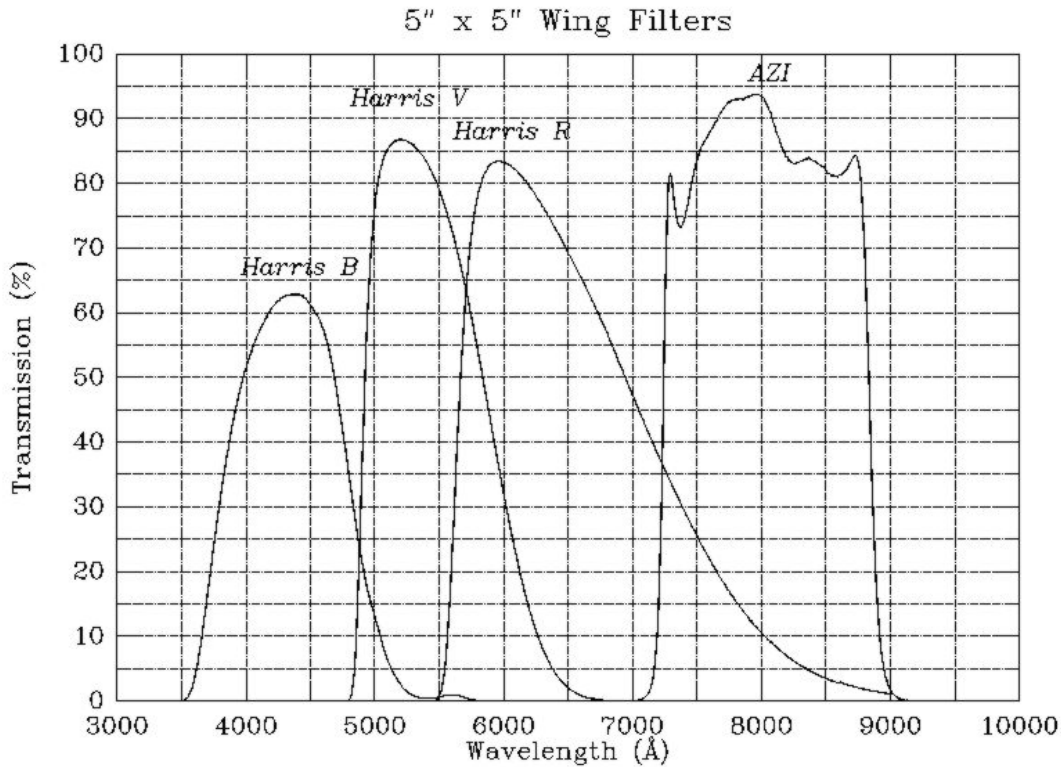


Figure 1. Filter bandpass tracings of available filters, including the Harris R band, as displayed on the james.as.arizona.edu 61'' telescope website.

The observation period began at 6:57:36.00 UT on February 26, 2022 and ended on 10:19:12.00 the same day. Because the target star and nearby reference objects were relatively faint, we used 30 second long exposures to ensure adequate counts for photometric comparison. To compensate for the long exposure time compared to the expected length of the transit from previous literature, we employed 3x3 pixel binning to reduce readout time, creating 1365x1365 px images. A total of 314 images were taken over the observation period, which were uploaded on the Nimoy supercomputer server system.

2.3 Preprocessing

Before differential photometry could be carried out, some images required automated or manual correction due to various atmospheric effects and artifacts. For example, image 66 contained a meteor streak across one of the reference stars, rendering the flux data unusable for that frame. In addition,

Dr. Green removed cosmic rays near the target star in images 5 and 29. Furthermore, due to the separation of the two halves of the CCD, overlap from overscan between halves had to be subtracted out, and dead columns on the CCD were interpolated over using a script on the observation site. After these corrections, we were left with 313 corrected images.

2.4 Image Processing and Differential Photometry

In order to obtain a light curve for K2-45 b, a differential photometry process was used to compare the target star brightness to nearby reference stars. The program AstroImageJ (AIJ) was used for image processing and aperture photometry (Collins et al. 2017). The 313 science images were loaded into AIJ’s CCD Data Processor Tool, which subtracted out the master bias and flat frames taken before the observations. This process corrected for noise associated with capturing the images and intrinsic brightness by pixel. We then utilized AIJ’s Multi Aperture Tool to visually display the processed science images and algorithmically generate radii for use in differential photometry comparisons. The program does this by plotting the brightness by pixel for a given distance about the selected point of the target star, known as the seeing profile, and automatically determining optimal thresholds to use for apertures. Using this process, the radius of the object aperture was set to 10.00 px (4.2” for 3x3 binning at 0.14 arcsec/pixel plate scale), with the inner and outer radii of the background annulus set to 18.00 (7.56”) and 27.00 pixels (11.34”). The signal from within the annulus, which corresponds to the background flux, is subtracted from the number of counts of the star. These radii were used to set apertures about the target star, which was located from a finder chart provided by Dr. Green, and apertures were additionally placed about 9 additional bright reference stars within the frame. Default settings were otherwise retained, and AIJ carried out the Multi-Aperture Photometry process, determining the relative change in brightness of our target over time compared to the comparison stars. The program generated a plot and table of the data, which were used for further analysis. To complete the remaining steps of the analysis, an XLS file containing transit data was transferred from the Nimoy system to a personal Windows system.

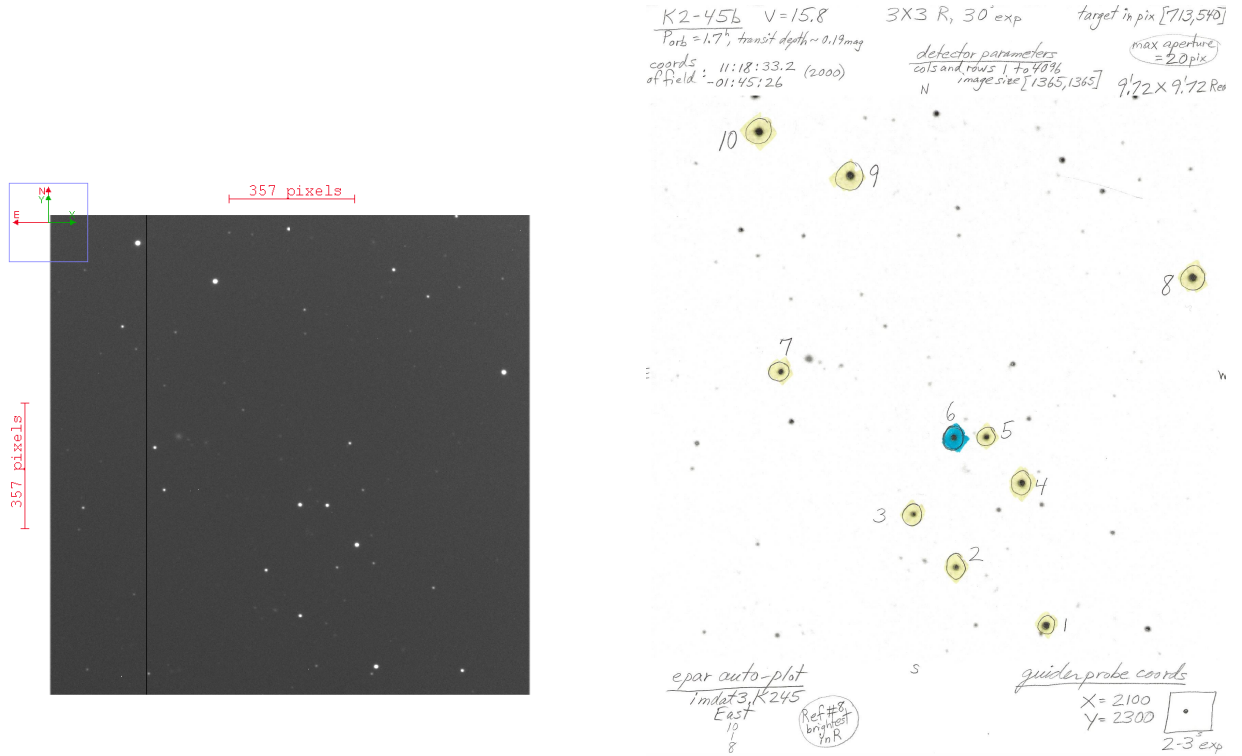


Figure 2. Example frame as displayed in AstroImageJ software after image processing and finder chart used to locate target star in frame

2.5 Model Fitting

An Anaconda Python Jupyter environment with NumPy and Matplotlib was used to extract, process, and plot the data from the AstroImageJ output file. Specifically, the extracted columns included the JD-2400000 (RJD) time, Target flux data, and Target flux error. We normalized the data by dividing flux and error values by the median of the out of transit data points, so that the baseline flux had a value of one, as seen in figure 3. Out of transit points were visually selected, with the first and last 80 flux values used for normalization.

Because the median of these values is being taken, erroneously omitting or including a small number points should have a negligible impact. The batman python package generates a transit light curve model from system parameters (Kreidberg 2015). From a single transit, the parameters we aimed to fit were the time of inferior conjunction (central transit time), planet radius and semi-major axis in stellar radii, and inclination of the system. The period of 1.729257 days and guess values for

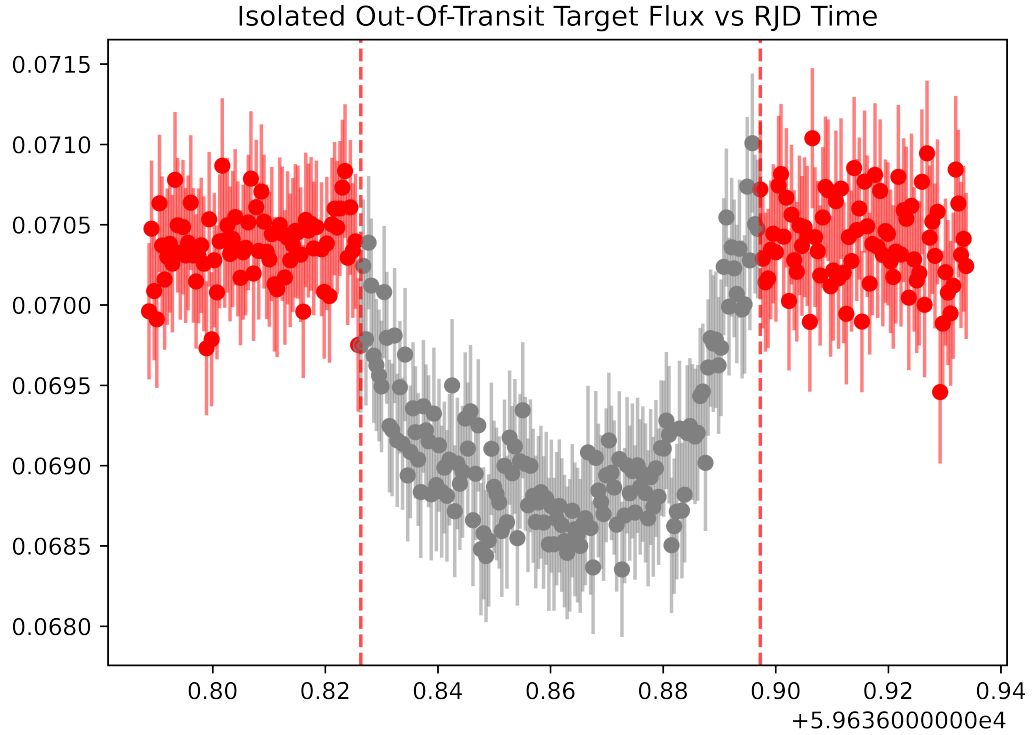


Figure 3. Plot of the out of transit flux data and flux error vs RJD used for normalization

the previously listed parameters were taken from Dressing et al. (2017). The time of central transit time guess value was taken as the midpoint of the observation period. We assume an eccentricity of 0 due to tidal circularization and an argument of periastron of 90° . Limb darkening parameters were generated by the EXOFAST Quadratic Limb Darkening applet (Eastman et al. 2013), which interpolates table values from Claret & Bloemen (2011). Specifically, we take an effective temperature from Dressing et al. (2017) and assume a metallicity of 0, which we justify by noting the similarity of K2-45 to our Sun in spectral type (via temperature). Wrapping these parameters in a light-curve generating function, we used SciPy’s least-squares curve fit optimization algorithm to fit the target parameters and produce a final best-fit model. The algorithm uses a least squares method with a grid search to test various values for the input parameters. The set of parameters which minimizes the sum of the squares of the distances from the model to the data is chosen as the optimal fit. The curve fit function also considers errors on the data to best constrain the fit to the observations. The

result of this fit overplotted with a batman model generated from the guess parameters from Dressing et al. (2017) is shown in Figure 4.

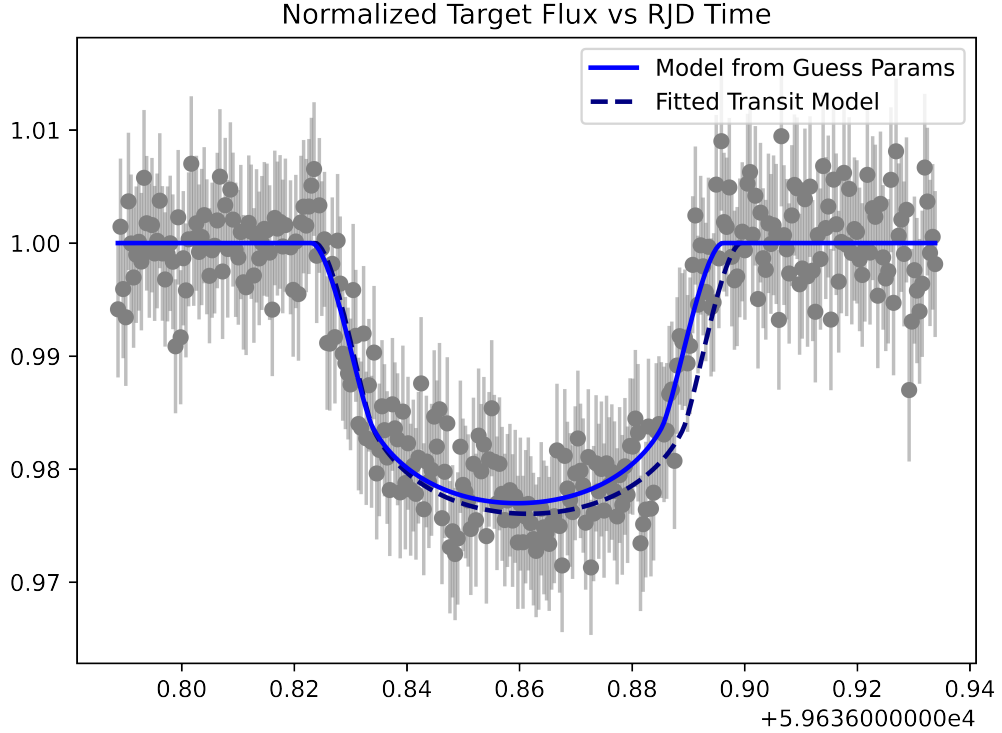


Figure 4. Plot of final fitted transit model over observation data overplotted with model generated from initial guess parameters

The fit visually looks accurate, but to conduct robust error analysis we generated a residual plot by subtracting fitted model values from the original data, as pictured in Figure 5. We present results from this analysis in Section 3.

3. RESULTS

By examining the fitted parameters returned by the curve fit function, we determine the physical and orbital characteristics for K2-45 b that best fit the observations. We find a time of central transit in RJD of 59636.859601, planet radius of 0.138632 and semi-major axis of 8.024 in stellar radii, and inclination angle of 86.97°. By taking a stellar radius of 0.685548 from Dressing et al. (2017), we compute K2-45 b to have a radius of 0.946133 R_J and a semi-major axis of 5.500944 R_\odot . The mean

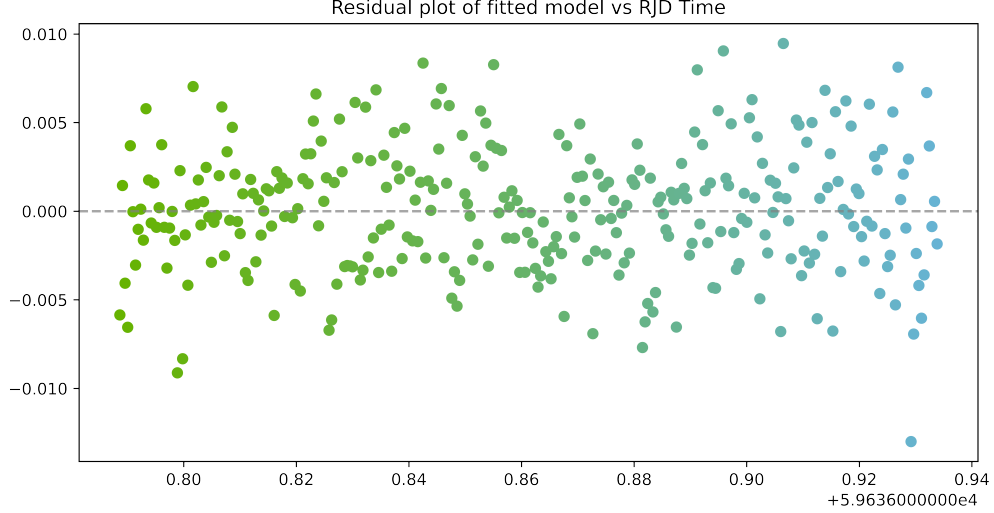


Figure 5. Residual plot between fitted model and normalized flux data

Table 1. Planet and Orbital Parameters Comparison with Literature

	R_P/R_{Jup}	$a(R_*)$	i
Best Fit Model	0.138632	8.02415629343442	86.97470403522962
Dressing et al. (2017)	0.139589	8.02	87.75
Percent difference	-0.6853566970475377	0.05182410766109629	-0.8835281649804889
Crossfield et al. (2016)	0.1376	7.18592	—
Percent difference	0.749273	11.664981	—

value of the residuals is 7.872e-05, which is negligible compared its spread, so the data is distributed roughly evenly about the fitted model. The standard deviation of the residuals is 0.0035438 compared to the mean on the normalized flux errors of 0.0060387. Because the former of these is smaller, we assert that the model is a good fit, as the average difference between the model and data is just over half the size of the error on the data itself.

4. SCIENTIFIC ANALYSIS AND DISCUSSION

Overall, we find a planetary radius slightly to moderately larger than the value presented in previous literature and a semi-major axis and inclination consistent with values from the Dressing et al. (2017)

paper. Our results for the best fit parameters of K2-45 b are consistent with a Hot Jupiter object, as the exoplanet orbits at an extremely close distance to its host star, which is comparable to the Sun, while remaining extremely massive compared to Solar System objects at a much greater orbital distance. We expect these objects to be over-represented in exoplanet transit surveys due to a relatively high transit depth, which is what we observed in our observations. A relatively large dip in brightness of the system was readily observable despite the low visual magnitude of the target star, use of a sub-optimal filter for the target, and the sparsity of nearby bright reference stars. Although our research did not focus on constraining the parameters of the host star of the K2-45 system, our group made a spectrographic observation of the star on April 9 using the Kitt Peak National Observatory 2.1-meter "Bok" Telescope located on Kitt Peak near Tucson, Arizona. Dr. Green additionally took spectra of several reference stars for comparison, allowing us to confirm our earlier analysis of the star as a K5 spectral type by overplotting the spectra of the reference star over that of our system and noting the close match between plots (Figure 6).

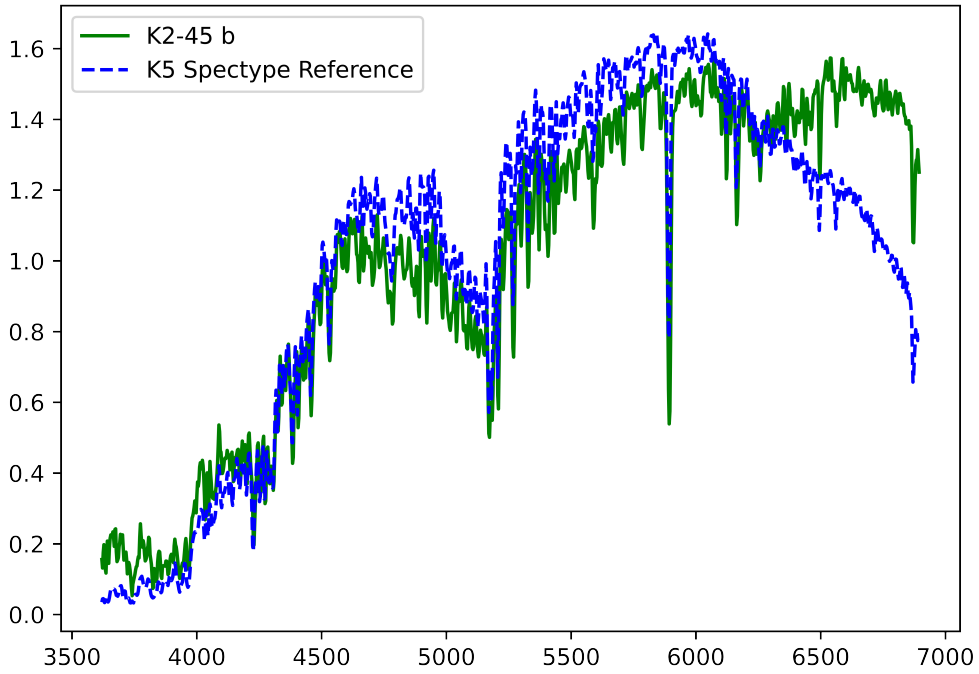


Figure 6. K2-45 b spectra overplotted by K5 spectral type reference star

5. CONCLUSION

Our team was successful in detecting an exoplanet in the K2-45 system relatively consistent with previous literature. By following a series of stages following an observation on the Mont4k CCD equipped 61" Kuiper telescope on Mount Bigelow, including manual and programmatic image correction; differential multi-aperture photometry; and transit model creation and curve fit optimization, our team was able to determine exoplanet characteristics and orbital parameters for K2-45 b, including radius, semi-major axis, and inclination. The results we produced were in general consensus with the previous literature, while we suggest that the radius of the exoplanet may be slightly larger than previously given within our error limits. We demonstrated that our final results represented a good fit on the data by providing analysis of residual data from the model on the original observations. We additionally commented on the significance of our results, as a further confirmation of a Hot Jupiter system, and provided brief commentary on an additional spectroscopic measurement taken

at a later date. As stated in the introduction, although this exoplanet does not have a chance of habitability, the value in this research is derived from the applicability of techniques in this study to other fields and in the study of the mechanics of other systems. Observations of extreme systems like these can lead to insight into the past and future development of the Solar System and other star systems throughout the Universe.

REFERENCES

- Ciardi, D. 2021, K2 Planets and Candidates Table, IPAC, doi: [10.26133/NEA19](https://doi.org/10.26133/NEA19)
- Claret, A., & Bloemen, S. 2011, A&A, 529, A75, doi: [10.1051/0004-6361/201116451](https://doi.org/10.1051/0004-6361/201116451)
- Collins, K. A., Kielkopf, J. F., Stassun, K. G., & Hessman, F. V. 2017, The Astronomical Journal, 153, 77, doi: [10.3847/1538-3881/153/2/77](https://doi.org/10.3847/1538-3881/153/2/77)
- Crossfield, I. J. M., Ciardi, D. R., Petigura, E. A., et al. 2016, ApJS, 226, 7, doi: [10.3847/0067-0049/226/1/7](https://doi.org/10.3847/0067-0049/226/1/7)
- Dressing, C. D., Vanderburg, A., Schlieder, J. E., et al. 2017, AJ, 154, 207, doi: [10.3847/1538-3881/aa89f2](https://doi.org/10.3847/1538-3881/aa89f2)
- Eastman, J., Gaudi, B. S., & Agol, E. 2013, PASP, 125, 83, doi: [10.1086/669497](https://doi.org/10.1086/669497)
- Gaia Collaboration, Brown, A. G. A., Vallenari, A., et al. 2018, A&A, 616, A1, doi: [10.1051/0004-6361/201833051](https://doi.org/10.1051/0004-6361/201833051)
- Kreidberg, L. 2015, PASP, 127, 1161, doi: [10.1086/683602](https://doi.org/10.1086/683602)
- Smith, P. 2022, The steward observatory 61" Kuiper telescope, University of Arizona Steward Observatory. <http://james.as.arizona.edu/~psmith/61inch/>
- Vanderburg, A., Latham, D. W., Buchhave, L. A., et al. 2016, ApJS, 222, 14, doi: [10.3847/0067-0049/222/1/14](https://doi.org/10.3847/0067-0049/222/1/14)